Theor Chem Acc (2011) 129:93–103
DOI 10.1007/s00214-011-0901-4

REGULAR ARTICLE

Reduction mechanism in class A methionine sulfoxide reductases: a theoretical chemistry investigation

E. Thiriot · G. Monard · S. Boschi-Muller · G. Branlant · M. F. Ruiz-López

Received: 25 January 2011 / Accepted: 29 January 2011 / Published online: 18 February 2011

Abstract Ab initio calculations at the B3LYP/6–311 ++G(2df,2p) and B3LYP/6–31G(d) level have been carried out to investigate the reaction mechanism of methionine sulfoxide reductases of class A. These enzymes reduce oxidized methionine in vivo and therefore play an important role in repairing protein damage caused by the oxidative stress. Our calculations have been carried out for a model reaction in a model active site. Several reaction mechanisms have been explored that can roughly be described as $(2H^+ + 2e^-)$ or $(H^+ + e^-)$. The results suggest that the actual reaction mechanism is of the $(2H^+ + 2e^-)$ type corresponding to a more or less asynchronous-concerted double-proton transfer reaction leading to the formation of methionine (dimethylthioether in our model) and a sulfenic acid Cys-SOH. The Michaelis complex would involve one deprotonated Cys and one protonated Glu residues in the active site, this protonation state being mandatory to stabilize the sulfoxide substrate. Then, proton transfer from Glu to the substrate takes place, followed by proton transfer from one Tyr residue and fast reorganization of the system. The overall activation energy barrier is estimated to fall in the range 7–9 kcal/mol, much lower than the predicted barrier in DMSO solution (29.6 kcal/mol) reported before.

Keywords Methionine sulfoxide reductase · Oxidative stress · Enzymatic catalysis · Sulfoxide · Ab initio calculations

1 Introduction

Oxidative stress may be the cause of protein damage involved in a variety of diseases and in aging process, most sensitive amino acids to oxidation being cysteine and methionine. The latter is converted into methionine sulfoxide, which can be reduced to restore the protein function by the so called methionine sulfoxide reductases (Msr) [1–14] There are two main classes of such enzymes, MsrA and MsrB. They display quite different structural forms but nevertheless share some analogies in the foremost stages of their reduction mechanism: specifically, both enzyme classes involve a catalytic cysteine, which is oxidized to sulfenic acid upon reduction of the substrate to methionine. In most Msrs, the sulfenic acid intermediate reacts with a recycling cysteine yielding an intramolecular disulfide bond that is further reduced by thioredoxin or thioredoxin-like proteins to complete the catalytic cycle. Scheme 1 summarizes the main steps of the Msr reaction mechanisms. Note that a new class of Msr (named fRMsr) not involved in protein repair has recently been discovered [15] whose catalytic mechanism is similar to that of MsrA and MsrB [16], i.e., it passes through the sulfenic acid chemistry.

The reduction reaction of a sulfoxide by a thiol has attracted attention in synthetic organic chemistry since many decades [17–24] and is well-known to be catalyzed

Electronic supplementary material The online version of this article (doi:10.1007/s00214-011-0901-4) contains supplementary material, which is available to authorized users.

E. Thiriot · G. Monard · M. F. Ruiz-López (✉)
Theoretical Chemistry and Biochemistry Group,
SRSMC, Nancy University, CNRS, BP 70239,
54506 Vandoeuvre-lès-Nancy, France
e-mail: Manuel.Ruiz@cbt.uhp-nancy.fr

S. Boschi-Muller · G. Branlant
Molecular and Structural Enzymology Group,
AREMS, Nancy University, CNRS, BP 70239,
54506 Vandoeuvre-lès-Nancy, France

Scheme 1 Main steps of the Msr reaction mechanisms

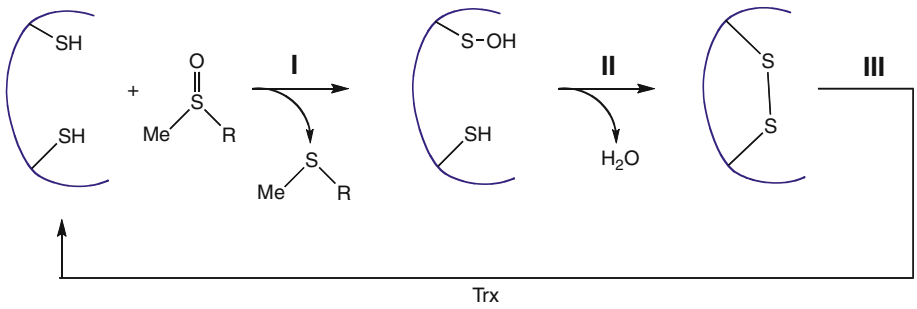

by acids, bases, amines [20, 21], halogen-hydrogen halides [22], metals [25–27], and alumina [28] for instance. The mechanism in solution was experimentally investigated by Wallace [18] and Wallace and Mahon [19], who pointed out that the activation energy is correlated with the pK_a of the thiol. Moreover, while the reaction was found to be overall second order, in the excess of one of the reagents, pseudo-first-order kinetics was observed.

The reaction between MeSH and DMSO in DMSO solution has been investigated with quantum chemical approaches too [29]. The proposed mechanism is summarized in Scheme 2. It involves the initial formation of a sulfurane intermediate through a stepwise mechanism in which proton transfer from the thiol to the sulfoxide is the rate determining step of the whole reduction mechanism, with activation free energy of 29.6 kcal/mol at 300 K (calculations at MP2/6–311 + G(3d2f,2df,2p)//B3LYP/6–311G(d,p) level of theory). Then, the sulfurane intermediate rapidly decays into the products. It reacts with another thiol molecule to yield sulfonium and thiolate ions that recombine to form either a sulfenic acid or a disulfide. The latter is much more stable than the former and is the only product experimentally observed in solution. This is not surprising since if a sulfenic acid is formed, fast decay to disulfide will probably take place in the presence of thiols, preventing the accumulation and thus the detection of the sulfenic acid intermediate.

The enzymatic mechanism would be expected to be similar to the chemical reaction in solution, but this hypothesis raises two important questions. First, the global activation barrier in solution is not compatible with the observed enzymatic rates, and the catalytic role of the enzyme needs to be clarified. Second, in solution, two protons are transferred from two different thiol molecules. In the enzymatic process, the first proton donor can be ascribed to the catalytic cysteine (see below however) but clearly the second one cannot be provided by the recycling cysteine, as biochemical and enzymatic studies showed that the sulfenic acid intermediate is still efficiently formed in its absence [2, 6]. On the other hand, one cannot definitively exclude that a different mechanism applies in the enzyme and in DMSO solution since the interaction of the chemical system with its environment does certainly produce major effects on the reaction.

In order to get a deeper insight on the Msr reaction mechanism, we have carried out a theoretical investigation of a model process in a model active site using quantum chemical calculations. We focus on the reduction step, i.e., on the passage from the initial sulfoxide entity to the reduced methionine plus a sulfenic acid.

2 Models and methods

One specific problem associated with the modeling of Msr reactivity (in contrast to other enzymes) is the lack of experimental data for equivalent processes in aqueous solution. The reduction of DMSO by thiols in DMSO solution is obviously a useful reference but the enzymatic mechanism cannot be directly inferred from it. On the one hand, sulfenic acid intermediates were not evidenced in experimental studies in DMSO due to their high chemical reactivity (if formed, the sulfenic acid should react with a second thiol molecule preventing its accumulation). On the

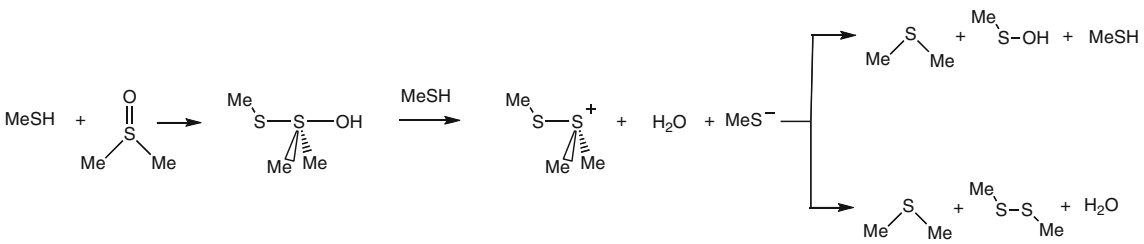

Scheme 2 Proposed mechanism for the MeSH + DMSO reaction in DMSO solution

other hand, the reduction mechanism in solution, which includes formation of the disulfide, appears to involve two thiol molecules, while only one Cys is involved in the enzymatic reduction reaction. Therefore, in order to get a deeper insight into Msr reactions, it is necessary to explore different mechanisms for processes including ionic or radical species, proton or electron transfer, etc. This is the aim of our study, in which three main reaction paths are analyzed and compared.

Unfortunately, since the total number of computations to do is quite large (several potential energy surfaces must be explored in detail), such kind of investigations cannot be carried out at a very high level of theory and/or using very elaborated protein models. The approach proposed here represents a compromise between accuracy and computational cost. Basically, we study the reaction mechanism in a model active site of the enzyme, with explicit representation of the amino acid side chains expected to play an active role in the process and a dielectric approach for the rest of the enzyme. This approach can be compared to the usual discrete-continuum method often employed for bulk solvent reactions. This scheme has some obvious limitations but there are two arguments supporting it: (1) it allows carrying out quantum mechanical calculations at a relatively high level (in particular for energy calculations) and (2) it may allow to exclude those mechanisms for which energy requirements are too large (see below), as more elaborated models should not change the conclusions. Finally, it should be noticed that this scheme has also been successfully used in the literature to study other enzymatic reactions.

Quantum mechanical calculations for the model active site described below have been carried out using the hybrid density functional method B3LYP [30, 31]. The potential energy surface is first explored using the 6–31G(d) basis set. Energy minima and transition structures are then located and verified by a standard vibrational analysis. Afterward, electronic energies are computed using the 6–311 ++G(2df,2p) basis set with long-range electrostatic effects being accounted for by the polarizable continuum model (PCM) approach [32, 33]. Net atomic charges are computed using the CHELPG method [34] and bond orders using the Mayer formalism [35]. All the calculations have been carried out using the Gaussian 03 package [36].

As said above, the active site model (Fig. 1) is limited to residues that were shown to play a role in MsrA catalysis [37]. They have been identified on the basis of the three-dimensional structure of the MsrA from *Escherichia coli* in covalent complex with cacodylate [3] and kinetics of mutated MsrAs [37] together with preliminary molecular dynamics simulations for the system [38]. The structure in reference [3] is a good mimic of the Michaelis complex: first, one of the two methyl groups of the cacodylate well

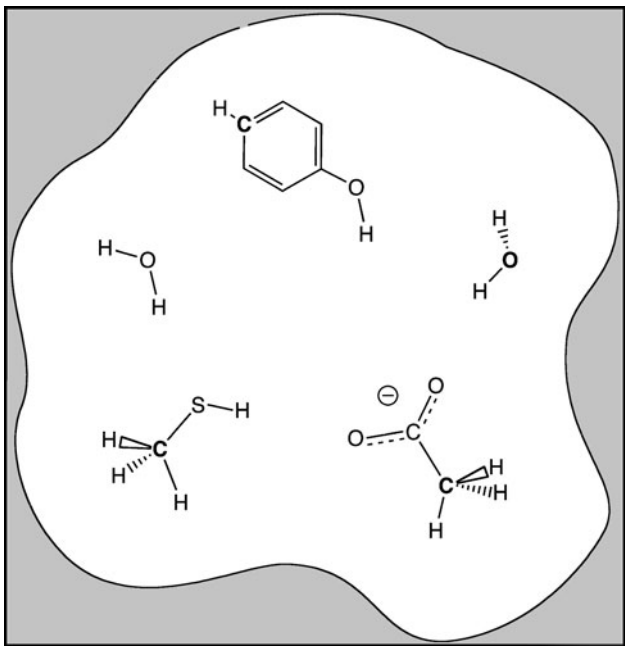

Fig. 1 Schematic active site model used in this study. The protonation state of the ionizable residues is chosen arbitrarily but corresponds to measured pK_a for Cys51 and estimated pK_a for Glu94 in the free enzyme, see Sect. 3. The position of *bold* atoms is fixed in geometry optimizations

represents the ε-methyl of the methionine sulfoxide, while the oxygen of the water molecule and As^{3+} mimics the oxygen and the sulfur atoms, respectively, and second, the geometry of the covalent adduct is tetrahedral like the sulfoxide function. Residues in the model therefore include Cys51, Glu94, Tyr134, and Tyr82 and have been modeled by, respectively, CH_3SH, CH_3COOH, PhOH, and H_2O. The choice of a water molecule for Tyr82 allows reducing the computational cost and has been made after considering the following experimental data. Only one Tyr is involved in the reductase step, since substituting either Tyr134 or Tyr82 by Phe leads to small or no rate effect at all, while substituting both tyrosine leads to a drastic decrease in the kinetics of the reductase step [37]. In other words, one Tyr can substitute the other for its role in catalysis. Hence, a minimal active site model requires including only one of the two Tyr, the other one being replaced by a water molecule. In addition to the above species, a second explicit H_2O molecule has been considered in our model to account for the presence of water in the active site, as shown in some crystallographic structures [39] and in MD simulations [38]. Finally, the DMSO molecule has been considered as a suitable model for methionine sulfoxide (actually, MsrA is able to reduce DMSO although less efficiently).

As usual when dealing with simple active models, the position of some atoms is fixed in order to account for the

constraints that are inherent to the true active site. Several strategies have been employed in the literature. Our choice was based on preliminary calculations of the system without constraints by verifying that calculations with the constraints described in the paper do not lead to very different results (especially in terms of comparison between mechanisms). In other words, we have verified that our constraints do not introduce unphysical terms. The strategy consisting in keeping frozen the α-carbon atoms would introduce larger flexibility in the system but it would represent a significant increase in computational time without significant improvement of the reaction energetics. Note that the DMSO molecule has no constraints and is therefore allowed to interact with the active site in the most favorable orientation. In the real enzyme, the hydrophobic pocket (namely Trp53 and Phe52) guides the orientation of the substrate and we have verified that the orientation of DMSO in our computations is consistent with that orientation.

3 Results and discussion

3.1 The Michaelis complex structure

We first consider the structure of the Michaelis complex, which will be defined here as the complex formed by the model active site and a DMSO molecule. Prior to the study of such a complex, few remarks concerning the protonation state of the ionizable residues need to be made.

In the free enzyme, the situation drawn in Fig. 1 is the most reasonable one. It corresponds to the expected pK_a values for Cys51 and Glu94. The experimental value reported by Antoine et al. [37] for Cys51 in the free MsrA from *Neisseria meningitidis* is 9.5 while the determination for Glu94 was not performed. Estimations using the PROPKA program [40–42] provides a pK_a value between 8.7 and 9.6 for Cys51, in very good agreement with experimental data, and 6.4 for the carboxylate of the side chain of Glu94, which is significantly higher than that in solution, i.e., 4.1.

In the Michaelis enzyme–substrate complex, the pK_{app} values of the catalytic Cys51, of the other amino acids involved in the chemistry of the reaction (Glu94, Tyr82, and Tyr134) and of the sulfoxide function of the substrate, likely undergo substantial changes to favor the catalytic efficiency of the reductase step. Evidence comes from the pH dependence of the rate constant of the reductase step, which is associated with the proton transfer from Cys51 to the sulfoxide function via Glu94. Indeed, the curve shows a monosigmoidal profile with a pK_{app} of 5.7 that was attributed to Cys51 [37]. Hence, when the Michaelis complex forms, the Cys51 pK_a experiences a drastic decrease, from 9.5 to 5.7. Surprisingly, Glu94, which was postulated to favor the hydrogen transfer from Cys51 to the oxygen of the sulfoxide [43], was not apparently titrated. Quite probably, this results from the fact that the pK_{app} of Glu94 should be quite close to the unusually low pKa of Cys51 in the enzyme–substrate complex.

On the other hand, the analysis of the crystallographic structure of MsrA in complex with the substrate [39] shows that (1) the oxygen atom of the sulfoxide function interacts by hydrogen bonding with Tyr82 and Tyr134, and (2) the distance of 2.5 Å between the sulfoxide O atom and the $O^{\varepsilon 2}$ of Glu94 corresponds to formation of a strong hydrogen bond and, thus, implies proton sharing between the two atoms. Finally, chemical considerations suggest that the protonation state of the active site in the Michaelis complex should differ from that in the free enzyme in solution to stabilize the strong dipole moment of the sulfoxide function. All these remarks support the schematic model displayed in Fig. 2 for the Michaelis complex. The optimized structure **1** is also shown in the Figure. As shown, the oxygen atom of the sulfoxide is involved in three hydrogen-bond interactions (with PhOH, H_2O and CH_3COOH). Other geometrical and electronic parameters for the system are summarized in Table 1. This table contains also data for the structures described hereafter along the reaction path.

3.2 The $2H^+ + 2e^-$ reduction mechanism

As said above, the reduction of sulfoxides by thiols in the absence of specific catalysts was theoretically investigated by Balta et al. [29]. They suggested a mechanism in which DMSO globally gets two protons and two electrons to yield one dimethylthioether and one water molecule. In their study, they have shown that this reaction starts by proton transfer from the thiol to the sulfoxide. In principle, this is not a quite favorable process because of the low acidity of thiols and the small proton affinity of sulfoxides (the pK_a of protonated DMSO is about −2), and accordingly, the activation energy in DMSO solution was predicted to be quite large. In the Michaelis complex, however, two factors might help reduce the energy requirements for sulfoxide protonation. On the one hand, the process involves proton donation by a slightly acidic group, Glu94. On the other hand, the protonated sulfoxide should considerably be stabilized, mainly by strong electrostatic interactions with the negative charges on Glu94 and Cys51. Exploration of the B3LYP potential energy surface for such a proton transfer in our model active site shows that the reaction intermediate **2** (Fig. 3; Table 1) exhibits a sulfurane-type structure with a trigonal bipyramidal geometry. In other words, the capture of the proton by DMSO spontaneously leads to the formation of a weak S–S bond. Figure 3

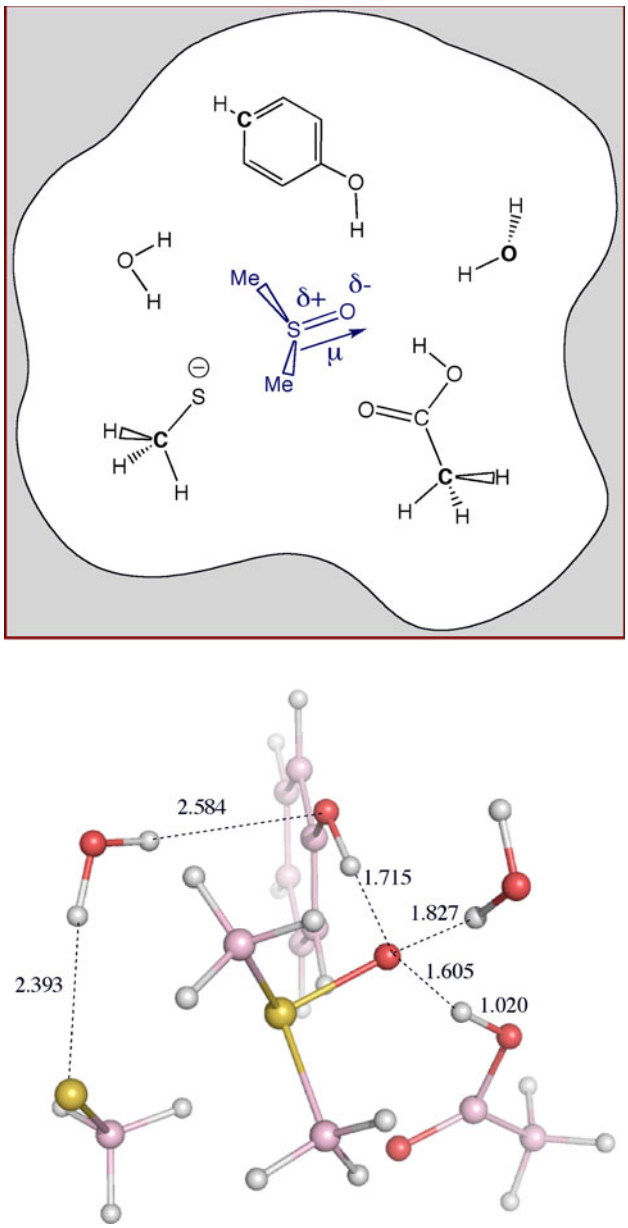

Fig. 2 Michaelis complex. *Up* schematic structure of DMSO in the model active site. *Down* optimized structure **1** at B3LYP level (the position of bold atoms has been constrained)

describes also the transition structure $\mathbf{TS_{1-2}}$ connecting **1** and **2**.

The S–S bond formation contributes to stabilize the system by redistributing the excess electronic charge on Cys51 and represents, as will become more apparent in the following, a key factor within the MsrA reaction mechanism. The energy of **2**, relative to the Michaelis complex, amounts only 5.6 kcal/mol, which can be compared with the approximately 9 kcal/mol required for a proton transfer from acetic acid to DMSO in bulk water (as deduced from experimental pKa's). The transition structure $\mathbf{TS_{1-2}}$ exhibits a similar energy (actually its structure is very close

Table 1 Some structural and electronic parameters computed for the Michaelis complex **1** and other relevant structures in the reduction reaction path described in this work (see Figs. 2, 3, 4, 5). The atomic coordinates for all the structures are provided as Electronic Supplementary Material

	1	$\mathbf{TS_{1-2}}$	**2**	$\mathbf{TS_{2-3}}$	**3**	**4**
Bond distances						
S–S	2.966	2.609	2.576	2.305	2.182	–
S–O	1.634	1.794	1.816	2.147	2.389	1.687[a]
S–S–O bond angle	166.2	170.5	170.9	177.4	173.1	–
Net atomic charges						
S_{thiol}	−0.79	−0.64	−0.61	−0.33	−0.24	−0.03
$S_{sulfoxide}$	0.74	0.59	0.56	0.48	0.51	−0.25
SS bond order	0.21	0.46	0.49	0.72	0.87	–

Geometries in Å and degrees, electronic parameters in atomic units

[a] SO bond in the sulfenic acid

to **2**, see Fig. 3 and Table 1), and therefore, the formation of the sulfurane-type intermediate in the active site of MsrA is a straightforward process (much easier than in DMSO reduction by thiols in solution, for which the activation energy has been evaluated at 19.3 kcal/mol [29]).

It is difficult to estimate the effective pK_{app} of the sulfurane intermediate in the active site (PROPKA calculations are not feasible in this case). However, experimental data for the MsrA reductase step k_{max} as a function of pH (see Fig. 3 in reference [37]) show that the optimum value is reached slightly above pH = 7 and remains optimal until pH = 9. This means that if the sulfurane species is to be formed, as suggested by our study, the associated pK_{app} value in the active site would be at least 9. It is worth noting that according to calculations, deprotonation of the sulfurane leads to S–S bond rupture. In that case, one expects the Michaelis complex to dissociate and the initial enzyme state SH/Glu^- to be recovered.

For completeness, it is interesting to stress that the S–S bond length is relatively large. Actually, the results show that the bond order related to the S–S bond is small (see Table 1), and therefore, the structure **2** can be viewed as a quite floppy intermediate. Besides:

- as usual in sulfuranes, the axial ligands are the most electronegative ones since this situation stabilizes the occupied antibonding orbital [29],
- any stationary point was found for a sulfurane with either the –OH or the $–SCH_3$ groups in the equatorial position (in both cases, geometry optimization leads to dissociation, see further comments below).

The question now is how the sulfurane intermediate **2** evolves to release a dimethylthioether molecule achieving

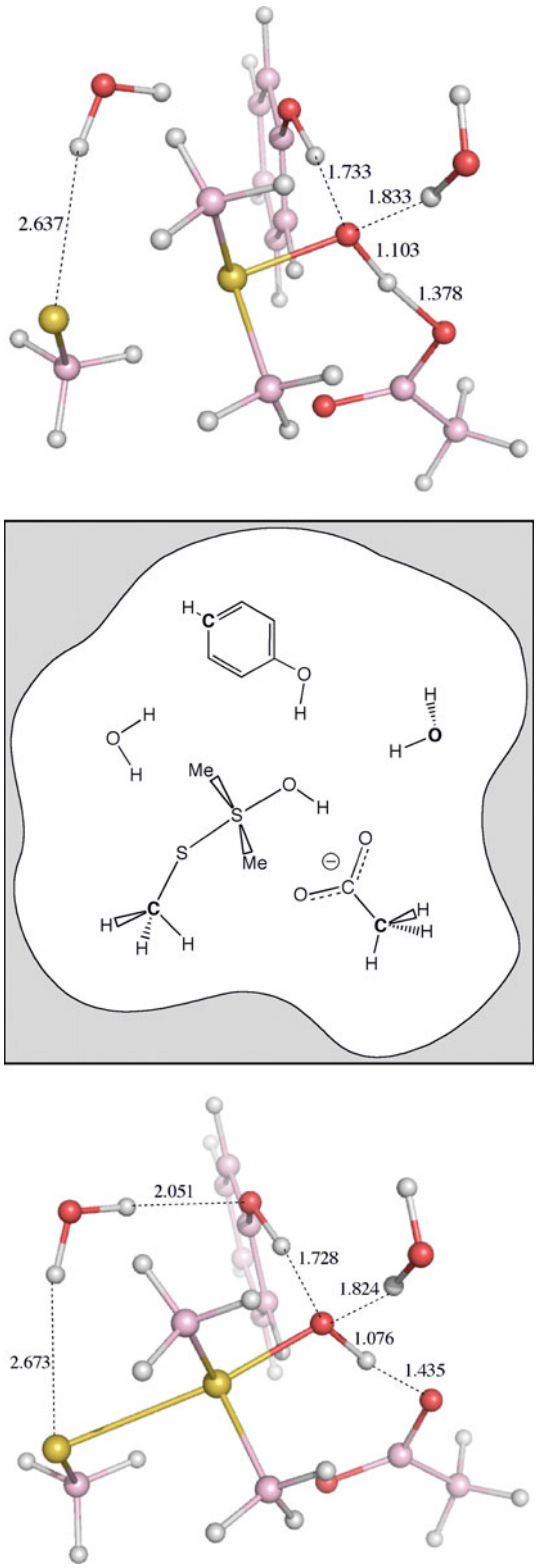

Fig. 3 Schematic geometry of **2** (*middle*) corresponding to protonation of DMSO in the model active site. B3LYP-optimized structures for $\mathbf{TS_{1-2}}$ (*up*) and **2** (*down*) (the position of *bold* atoms has been constrained). Relative energies with respect to **1** are 5.6 kcal/mol for both $\mathbf{TS_{1-2}}$ and **2**

in this way the reduction of DMSO. In solution, according to a previous theoretical study [29], a second thiol molecule protonates the sulfurane OH group and initiates the process [29]. It provokes the dissociation of **2** into a water molecule and a sulfonium ion that subsequently undergoes extremely fast hydrolysis to yield the dimethylthioether and a sulfenic acid. As already pointed out, studies on Msrs including not only MsrA but also MsrB and fRMrs [16] demonstrated formation of a sulfenic acid intermediate in the reduction step before formation of the disulfide intermediate (Scheme 1).

If we assume an enzymatic mechanism similar to the chemical mechanism in solution, the potential proton donors located in the proximity of the sulfurane intermediate in the MsrA active site are Tyr134, Tyr82, or water (see W1 and W2 in Fig. 4 of reference [39]). Nevertheless, acidity considerations point in favor of one of the tyrosines as proton donor. We have investigated the corresponding reaction path, and the calculations reveal that proton transfer from phenol (Tyr134) to the OH sulfurane group is relatively easy. As expected, formation of a water molecule and a sulfonium ion is obtained. The optimized structure **3** and the transition structure $\mathbf{TS_{2-3}}$ are drawn in Fig. 4 (see also Table 1). Relative energies with respect to **1** are 3.8 kcal/mol and 7.0 kcal/mol, respectively. Some parameters are gathered in Table 1. Since, as said above, the hydrolysis of the sulfonium ion is expected to be extremely fast, one can consider that **3** leads spontaneously (or through a small activation barrier) to the free thioether and the sulfenic acid derivative **4** shown in Fig. 5, although formally we have not located a transition state $\mathbf{TS_{3-4}}$ connecting them. Two remarks can be done here. The first one is that the formed water molecule interacts with the tyrosinate and carboxylate anions in **3** through strong hydrogen bonds, and therefore, it is activated to produce the nucleophilic attack on the sulfonium cation. Second, the question arises of whether the same water molecule formed through protonation of the sulfurane actually attacks the sulfonium cation. Moreover, the formation of this water molecule and its subsequent attack to the sulfonium yielding a sulfenic acid might be produced in a globally single reaction step because, as said, the second part of the process is expected to be quite fast. If that is the case, the oxygen atom of the sulfenic acid should be that on the initial sulfoxide function and in principle, this could be evidenced by isotopic labeling experiments (work is in progress).

The whole reaction profile is presented in Fig. 6. We report three curves. The first one does not take into account the influence of environment beyond the active site (isolated active site, energies presented above). In the other curves, we have made a rough estimation of the stabilizing

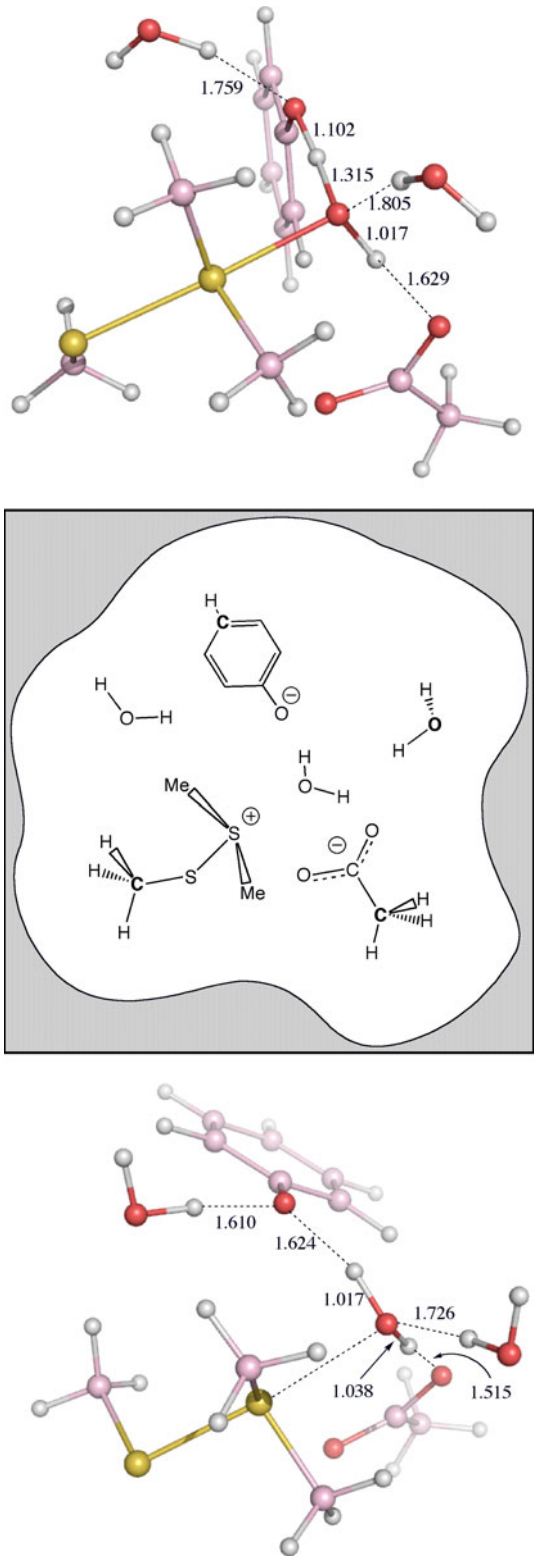

Fig. 4 Schematic geometry of **3** (*middle*) corresponding to proton transfer from PhOH (Tyr134) to the OH group in the sulfurane species. B3LYP-optimized structures for $\mathbf{TS_{2-3}}$ (*up*) and **3** (*down*) (the position of bold atoms has been constrained). Relative energies with respect to **1** are 7.0 kcal/mol and 3.8 kcal/mol, respectively

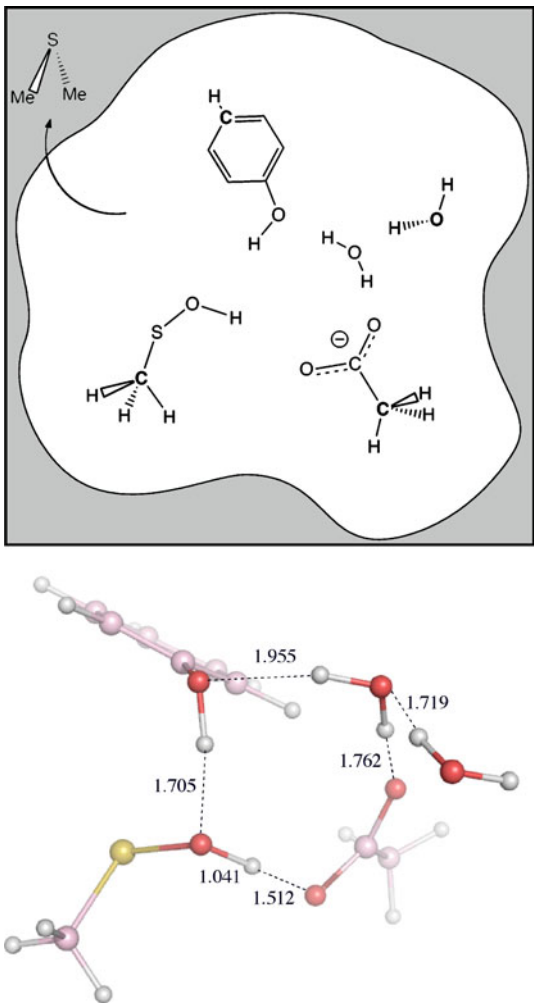

Fig. 5 Schematic geometry (*up*) corresponding to the product of the reaction (**4**+ dimethylthioether) with a sulfenic acid in the active site and B3LYP-optimized structures for **4** (*down*) (the position of bold atoms has been constrained). Relative energy with respect to **1** is −12.4 kcal/mol

effect due to long-range dielectric effects. For this purpose, we use the PCM model: the model active site is assumed to be surrounded by a medium having a dielectric constant equal 2 (apolar, polarizable medium) or 78.4 (the value for liquid water). The geometry is taken from the isolated active site without further optimization. The effective dielectric constant of the environment in the enzyme is expected to be intermediate between these values, which can therefore be considered as lower and upper limits for the dielectric effect. More accurate calculations could be done using explicit models such as the combined QM/MM molecular dynamics approach, but such a refinement was beyond the objectives of the present work.

As said above, if one considers the energy profile for the isolated active site, one sees that the sulfurane structure **2** and the intermediate **3** correspond to very shallow energy

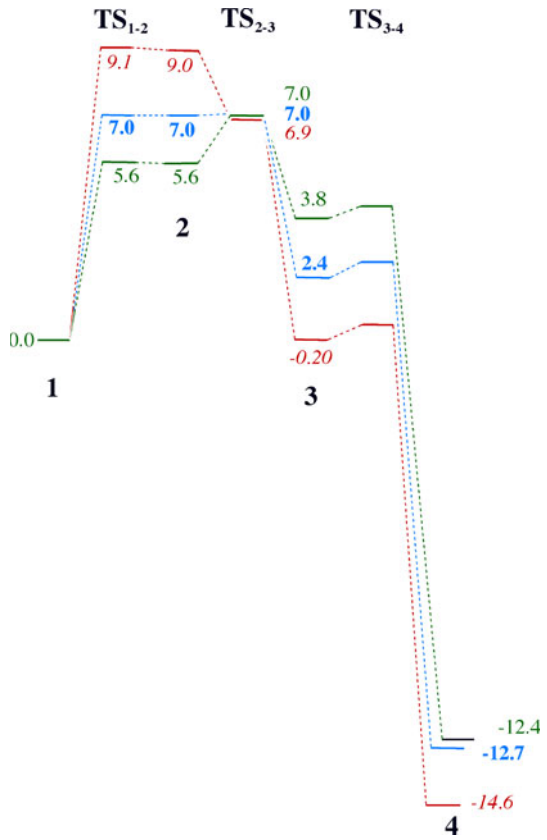

Fig. 6 Potential energy surface along the reaction path for DMSO reduction in the model active site of MsrA. Structure **TS_{3-4}** was not located in the active site but according to previous calculations (see text), the associated activation barrier should be quite small. Calculated energies (in kcal/mol) for the model active site without environmental effects (*green*, *roman*) and with environmental effects obtained using a dielectric constant of 2 (*blue*, *bold*) or 78.4 (*red*, *italics*)

minima. Thus, roughly, the whole reduction process can be described by an asynchronous-concerted double-proton transfer process in the Michaelis complex involving two proton donors, Glu94 and Tyr134 (or Tyr82). The second proton transfer, the one going through **TS_{2-3}**, determines the activation barrier, which is close to 7 kcal/mol and is therefore much lower than the estimated barrier in solution (29.6 kcal/mol).

When the dielectric effect of the medium is accounted for, the process is still described by an asynchronous-concerted double-proton transfer. However, the relative position of **TS_{1-2}** and **TS_{2-3}** changes. In the apolar medium, the two TSs and the sulfurane intermediate exhibit very close energies. In the polar one, the reaction rate is mainly controlled by the first proton transfer occurring after the Michaelis complex formation, i.e., the transfer from Glu94 to the sulfoxide. In the later medium, the whole activation energy is slightly higher and close to 9 kcal/mol, but still much lower than the activation barrier in DMSO solution. In both cases, the sulfurane **2** can be associated to the transition structure since, roughly, it lies at the top of the potential energy curve and it geometry is close to that of **TS_{1-2}**.

This reaction mechanism is consistent with the fact that substituting both Tyr82 and Tyr134 by two Phe residues in the MsrA from *N. meningitidis* led to a drastic decrease in the rate of the reductase step, i.e., a factor 10^4 while substituting only one of these tyrosines led to no significant rate effect for Y134F MsrA or only a small effect for Y82F MsrA. These results support the idea that both tyrosines can play the role of proton donor so that when only one is substituted, the other one can play its catalytic role.

3.3 Exploring other DMSO reduction mechanisms

Let us examine now other hypothesis for the reaction path. The simplest one consists of an OH group transfer and is inspired from previous theoretical studies for the peroxide + thiolate [44, 45] and DMSO + thiol [29] reactions. As in the $2H^+ + 2e^-$ mechanism, this mechanism starts by DMSO protonation and formation of the sulfurane (**2** in Fig. 3). In the subsequent step, the latter molecule undergoes a geometrical deformation so that the –OH and $–SCH_3$ groups become closer and are allowed to interact. The process leading to the sulfenic acid from the sulfurane is schematized in Scheme 3. Formally, in this mechanism and in contrast to the previous one, only one proton is transferred from Cys51 to the oxygen of the sulfoxide via Glu94. Tyr 82 and Tyr134 would not play the role of bases and would not be directly involved in the process, their main role here being the stabilization of the Michaelis complex.

The conformation of the sulfurane has to change considerably since initially the –OH and $–SCH_3$ groups occupy

Scheme 3 Sulfenic acid formation from sulfurane through a hypothetical OH transfer mechanism

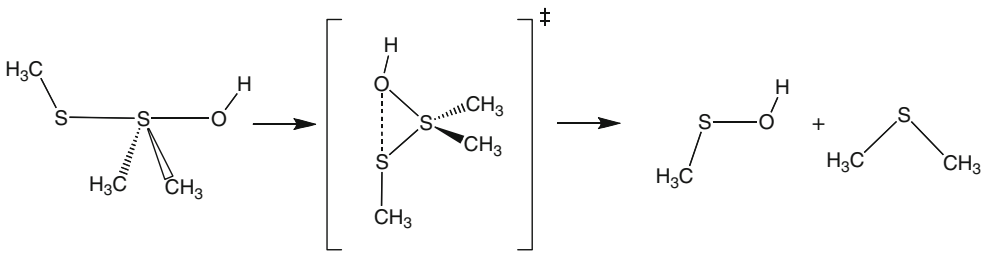

the axial positions (see Scheme 3 and structure **2** in Fig. 3). A transition state of this type for the isolated sulfurane was reported before and was shown to involve considerable activation energy (about 40 kcal/mol [29]). Attempts to locate a similar transition state within the active site going from the sulfurane to the sulfenic acid intermediates in the enzyme active site model were unfruitful. In fact, in order to bring closer the –OH and $–SCH_3$ groups, the initially linear angle S–S–O has to decrease. A relaxed potential energy surface scan calculation with a constrained angle shows that this type of deformation produces sulfurane dissociation in a way equivalent to that obtained with the pseudo-rotation of $–SCH_3$ (bringing it to the equatorial position). In both cases, there is a concomitant proton transfer from the phenol group to the –OH group, and finally, one obtains a product similar to **3**. The associated energy profile, however, involves a higher barrier than the one obtained in the $2H^+ + 2e^-$ mechanism and will not be detailed here.

DMSO reduction might also happen via a $1H^+ + 1e^-$ scenario for which the formation of the dimethylthioether is accompanied by the production of a hydroxyl radical molecule. In the $2H^+ + 2e^-$ reaction mechanism above, a closed-shell wave function has systematically been assumed and this assumption might hide the existence of reaction paths involving radical species. In particular, upon DMSO protonation in the Michaelis complex, electron transfer from the Cys^- residue could be postulated leading to the formation of an open-shell diradical system. The sulfonium-type radical formed, however, is not stable, and calculations show that it dissociates to dimethylthioether and hydroxyl radical. The process can be written:

$$\begin{aligned} CH_3S^- + (CH_3)_2S - OH^+ &\rightarrow CH_3S\cdot + (CH_3)_2\dot{S} - OH \\ &\rightarrow CH_3S\cdot + (CH_3)_2S + \cdot OH \end{aligned} \quad (1)$$

The formed hydroxyl radical could then react very quickly with other species in the environment, in particular with the thiyl radical, to finally form a sulfenic acid CH_3S–OH. The relevant ionization potential and redox potentials in gas phase and aqueous solution have been computed, and the values are summarized in Table 2. Redox potentials have been computed according to Fu et al. [46] (the value for the thiyl/thiolate pair is consistent with available experimental data [47, 48]). Solvation in water is incorporated with the PCM model. An important contribution to the properties of $(CH_3)_2S–OH^+$ comes from geometry relaxation after electron capture, the difference between the adiabatic and vertical affinities (ΔE in Table 2) being as large as 31.9 kcal/mol.

The data clearly indicate that electron transfer defined by Eq. 1 is a quite exergonic process in gas phase, with $\Delta G = -95.1$ kcal/mol, and quite endergonic in aqueous solution, where $\Delta G = +23.7$ kcal/mol

Table 2 Adiabatic electron affinities of the oxidized form (ΔE, ΔH, and ΔG in kcal/mol), solvation energies of the reduced and oxidized forms (ΔG_{solv} in kcal/mol), and absolute redox potential (V) (for comparison, the best estimate for the absolute redox potential of hydrogen is 4.28 V [49–51])

	ΔE	ΔH	ΔG	ΔG_{solv} ox/red	E°
$CH_3S\cdot/CH_3S^-$					
Gas	−42.8	−44.0	−43.7		2.17
	−43.3				
Water			−109.0	−2.0/−67.3	5.01
$(CH_3)_2S–OH^+/(CH_3)_2S + \cdot OH$					
Gas	−135.7	−137.0	−138.8		6.30
	−103.8				
Water			−85.3	−62.0/−8.5	3.98

Vertical affinities (ΔE) are given in italics

In the enzymatic environment, the species are not at infinite separation and the associated ΔG does not necessarily reflect the predictions in bulk water since: (1) the direct interaction between the ions or radicals has to be considered and (2) the interactions of the complex with the environment are presumably much lower compared to separated species. The first remark suggests that electron transfer would be inhibited (preferential stabilization of the ionized system) while the second one suggests the opposite. An estimation of the vertical electron transfer energy (B3LYP/6–31G(d) calculations) for a complex separated by an S–S distance of 4 Å in the enzymatic environment leads to +85 kcal/mol, showing that environmental effects are predominant and significantly disfavor the radical $1H^+ + 1e^-$ mechanism. One must stress, before concluding, that the above values depend a lot on S–S distance, and in order to explore this mechanism further, an analysis of the adiabatic curves for the two electronic states, ionized and diradical, as a function of that distance would be important. To account for thermal fluctuations in the Michaelis complex, the quantum mechanical investigation should be coupled to statistical methods and here too the combined QM/MM molecular dynamics approach would be particularly well adapted.

4 Conclusions

The present calculations, although based on a relatively simple computational model, suggest a reduction mechanism of MsrAs corresponding to a double-proton transfer that can roughly be described as an asynchronous—concerted mechanism in a catalytic triad composed by Cys51, Tyr134 or Tyr82, and Glu94. The transition state geometry

resembles that of a trigonal bipyramidal sulfurane species (intermediate **2**). The activation energy is predicted to be about 7–9 kcal/mol at the B3LYP level employed here.

Another important point is the fact that the interaction of the enzyme with the sulfoxide substrate induces not only a modification of the ionization state of the active site that leads, in particular, to a drastic decrease in the pK_{app} of Cys51, but likely also a stabilization of the polarized form of the sulfoxide function. Formation of a competent enzyme–substrate complex would be thus substrate assisted. In agreement with this assumption is the fact that mutating Glu94, Tyr82, and Tyr 134 all together leads to a drastic decrease in the reductase step rate by a factor of 10^4 and to a drastic increase in the pK_{app} of Cys51, whose value becomes now similar to that found in the free enzyme i.e. 9.5.

Further work will be necessary to clarify a number of points, such as the role of the protein environment beyond the active site (modeled here by a polarizable dielectric continuum), the mechanism of initial ionization of the catalytic Cys, or the stability of the Michaelis complex postulated in our work. Moreover, the experimentally observed analogies and differences between MsrA and MsrB enzymatic mechanisms cannot be simply explained by extrapolating results from the present study and a separate study for MsrB will be required. Investigating the mechanism of the recently discovered fRMsr enzymes [15] will be important in this context too. As said above, though they only reduce free R-Me–O, they involve the sulfenic acid chemistry presumably using another acid–base catalyst, i.e., Asp [16] instead of Glu and His in MsrA and MsrB, respectively. The calculations reported here constitute a basic framework for carrying out future theoretical analysis on these systems.

Acknowledgments The authors thank the PRST "Bioingénierie" and the French Ministry of Research (ACI IMPBio program, project SIRE) for financial support. They also thank the French facility CINES for providing computational resources.

References

1. Lowther WT, Brot N, Weissbach H, Matthews BW (2000) Biochemistry 39:13307
2. Boschi-Muller S, Azza S, Sanglier-Cianferani S, Talfournier F, van Dorsselear A, Branlant G (2000) J Biol Chem 275:35908
3. Tête-Favier F, Cobessi D, Boschi-Muller S, Azza S, Branlant G, Aubry A (2000) Structure Fold Des 8:1167
4. Moskovitz J, Bar-Noy S, Williams WM, Requena J, Berlett BS, Stadtman ER (2001) Proc Natl Acad Sci USA 98:12920
5. Boschi-Muller S, Azza S, Branlant G (2001) Protein Sci 10:2272
6. Kumar RA, Koc A, Cerny RL, Gladyshev VN (2002) J Biol Chem 277:37527
7. Lowther WT, Weissbach H, Etienne F, Brot N, Matthews BW (2002) Nat Struct Biol 9:348
8. Olry A, Boschi-Muller S, Marraud M, Sanglier-Cianferani S, van Dorsselear A, Branlant G (2002) J Biol Chem 277:12016
9. Taylor AB, Benglis DM Jr, Dhandayuthapani S, Hart PJ (2003) J Bacteriol 185:4119
10. Antoine M, Boschi-Muller S, Branlant G (2003) J Biol Chem 278:45352
11. Kim H-Y, Gladyshev VN (2004) Mol Biol Cell 15:1055
12. Olry A, Boschi-Muller S, Branlant G (2004) Biochemistry 43:11616
13. Coudevylle NT A, Azza S, Boschi-Muller S, Branlant G, Cung M-T (2004) J Biomol NMR 30:363
14. Boschi-Muller S, Olry A, Antoine M, Branlant G (2005) Biochim Biophys Acta 1703:231
15. Lin Z, Johnson LC, Weissbach H, Brot N, Lively MO, Lowther WT (2007) Proc Natl Acad Sci USA 104:9597
16. Gruez A, Libiad M, Boschi-Muller S, Branlant G (2010) J Biol Chem 285:25033
17. Yiannios CN, Karabinos JV (1963) J Org Chem 28:3246
18. Wallace TJ (1964) J Am Chem Soc 86:2018
19. Wallace TJ, Mahon JJ (1964) J Am Chem Soc 86:4099
20. Wallace TJ, Mahon JJ (1965) J Org Chem 30:1502
21. Epstein WW, Sweat FW (1967) Chem Rev 67:247
22. Lowe OG (1975) J Org Chem 40:2096
23. Lowe OG (1976) J Org Chem 41:2061
24. Madesclaire M (1988) Tetrahedron 44:6537
25. Arterburn JB, Perry MC, Nelson SL, Dible BR, Holguin MS (1997) J Am Chem Soc 119:9309
26. Abu-Omar MM, Khan SI (1998) Inorg Chem 37:4979
27. Arnáiz FJ, Aguado R, Pedrosa MR, De Cian A (2003) Inorg Chim Acta 347:33
28. Hirano M, Yakabe S, Monobe H, Morimoto T (1998) J Chem Research (S) (8):472–473
29. Balta B, Monard G, Ruiz-López MF, Antoine M, Gand A, Boschi-Muller S, Branlant G (2006) J Phys Chem A 110:7628
30. Becke AD (1993) J Chem Phys 98:5648
31. Lee C, Yang W, Parr RG (1988) Phys Rev B 37:785
32. Tomasi J, Bonaccorsi R, Cami R, Olivares del Valle FJ (1991) J Mol Struct Theochem 234:401
33. Tomasi J, Persico M (1994) Chem Rev 94:2027
34. Breneman CM, Wiberg KB (1990) J Comp Chem 11:361
35. Mayer I (1983) Chem Phys Lett 97:270
36. Frisch MJ, Trucks GW, Schlegel HB, Scuseria GE, Robb MA, Cheeseman JR, Montgomery Jr JA, Vreven T, Kudin KN, Burant JC, Millam JM, Iyengar SS, Tomasi J, Barone V, Mennucci B, Cossi M, Scalmani G, Rega N, Petersson GA, Nakatsuji H, Hada M, Ehara M, Toyota K, Fukuda R, Hasegawa J, Ishida M, Nakajima T, Honda Y, Kitao O, Nakai H, Klene M, Li X, Knox JE, Hratchian HP, Cross JB, Bakken V, Adamo C, Jaramillo J, Gomperts R, Stratmann RE, Yazyev O, Austin AJ, Cammi R, Pomelli C, Ochterski JW, Ayala PY, Morokuma K, Voth GA, Salvador P, Dannenberg JJ, Zakrzewski VG, Dapprich S, Daniels AD, Strain MC, Farkas O, Malick DK, Rabuck AD, Raghavachari K, Foresman JB, Ortiz JV, Cui Q, Baboul AG, Clifford S, Cioslowski J, Stefanov BB, Liu G, Liashenko A, Piskorz P, Komaromi I, Martin RL, Fox DJ, Keith T, Al-Laham MA, Peng CY, Nanayakkara A, Challacombe M, Gill PMW, Johnson B, Chen W, Wong MW, Gonzalez C, Pople JA (2004) Gaussian 03, revision C.02. Gaussian Inc., Wallingford
37. Antoine M, Gand A, Boschi-Muller S, Branlant G (2006) J Biol Chem 281:39062
38. Thiriot E (2008) Thesis, Nancy University, Vandoeuvre-lès-Nancy, France
39. Ranaivoson FM, Antoine M, Kauffmann B, Boschi-Muller S, Aubry A, Branlant G, Favier F (2008) J Mol Biol 377:268
40. Perrin DD, Dempsey B, Serjeant EP (1981) pKa Prediction for organic acids and bases. Chapman & Hall, London

41. Li H, Robertson AD, Jensen JH (2005) Proteins Struct Funct. Genet 61:704
42. Bas DC, Rogers DM, Jensen JH (2008) Proteins Struct Funct. Genet 73:765
43. Boschi-Muller S, Gand A, Branlant G (2008) Arch Biochem Biophys 474:266
44. Cardey B, Enescu M (2005) Chem Phys Chem 6:1175
45. Cardey B, Enescu M (2007) J Phys Chem A 111:673
46. Fu Y, Liu L, Yu H-Z, Wand Y-M, Guo Q-X (2005) J Mol Struct Theochem 127:7227
47. Forni LG, Willson RL (1986) Biochem J 240:897
48. Vorontsov AV (2008) Russ Chem Rev 77:909
49. Lewis A, Bumpus JA, Truhlar DG, Cramer CJ (2004) J Chem Educ 81:596
50. Lewis A, Bumpus JA, Truhlar DG, Cramer CJ (2007) J Chem Educ 84:934
51. Kelly CP, Cramer CJ, Truhlar DG (2007) J Phys Chem B 111:408